Basaltic calderas: Collapse dynamics, edifice deformation, and variations of magma withdrawal

Laurent Michon, Frédérick Massin, Vincent Famin, Valérie Ferrazzini, Geneviève Roult

Basaltic calderas: Collapse dynamics, edifice deformation, and variations of magma withdrawal

Laurent Michon,[1,2,3] Frédérick Massin,[2,3,4] Vincent Famin,[1,2,3] Valérie Ferrazzini,[2,3,4] and Geneviève Roult[3,5]

Received 14 April 2010; revised 29 November 2010; accepted 4 January 2011; published 31 March 2011.

[1] The incremental caldera collapses of Fernandina (1968), Miyakejima (2000), and Piton de la Fournaise (2007) are analyzed in order to understand the collapse dynamics in basaltic setting and the associated edifice deformation. For each caldera, the collapse dynamics is assessed through the evolution of the (1) time interval *T* between two successive collapse increments, (2) amount of vertical displacement during each collapse increment, and (3) magma outflow rate during the whole collapse caldera process. We show from the evolution of *T* that Piton de la Fournaise and Fernandina were characterized by a similar collapse dynamics, despite large differences in the caldera geometry and the duration of the whole collapse caldera process. This evolution significantly differs from that of Miyakejima where *T* strongly fluctuated throughout the whole collapse process. Quantification of the piston vertical displacements enables us to determine the magma outflow rates between each collapse increment. Displacement data (tiltmeter and/or GPS) for Piton de la Fournaise and Miyakejima are used to constrain the edifice overall deformation and the edifice deformation rates. These data reveal that both volcanoes experienced edifice inflation once the piston collapsed into the magma chamber. Such a deformation, which lasts during the first collapse increments only, is interpreted as the result of larger volume of piston intruded in the magma chamber than magma withdrawn before each collapse increment. Once the effect of the collapsing rock column vanishes, edifice deflates. We also determine for each caldera the critical amount of magma evacuated before collapse initiation and compare it to analog models. The significant differences between models and nature are explained by the occurrence of preexisting weak zones in nature, i.e., the ring faults, that are not taken into account in analog models. Finally, we show that *T* at Piton de la Fournaise and Fernandina was equally controlled by the frictional resistance along the ring faults and the magma outflow rate. In addition to these two parameters, the collapse dynamics of Miyakejima was also influenced by variations of the magma bulk modulus, which changed after the influx of deep gas-rich magma into the collapse-related magma chamber. Altogether, our results show that the dynamics of caldera collapse in basaltic volcanoes proceeds in two phases: Phase 1, starting with the first collapse, is characterized by the largest collapse amplitude, an incremental edifice inflation, and a step-by-step increase of the rate of magma outflow. Phase 2 shows a rapid decrease of the magma discharge rate to a low level concomitant with the continuous edifice deflation. If deep magma is injected into the magma chamber, as at Miyakejima, an additional phase occurs (phase 3).

Citation: Michon, L., F. Massin, V. Famin, V. Ferrazzini, and G. Roult (2011), Basaltic calderas: Collapse dynamics, edifice deformation, and variations of magma withdrawal, *J. Geophys. Res.*, *116*, B03209, doi:10.1029/2010JB007636.

1. Introduction

[2] One of the most striking features recorded during the recent formation of calderas at Fernandina (Galapagos, 1968), Miyakejima (Japan, 2000) and Piton de la Fournaise (La Réunion, 2007) is the incremental collapse of the rock column into the magma chamber [*Simkin and Howard*, 1970; *Kumagai et al.*, 2001; *Michon et al.*, 2007]. The mechanics of collapse is usually explained in terms of recurrent stress increase along the ring faults until failure of the country rocks [*Simkin and Howard*, 1970; *Kobayashi et al.*, 2003].

[1] Laboratoire GéoSciences Réunion, Université de la Réunion, Saint Denis, France.
[2] Institut de Physique du Globe de Paris, Sorbonne Paris Cité, Paris, France.
[3] UMR 7154, CNRS, Paris, France.
[4] Observatoire Volcanologique du Piton de la Fournaise, La Plaine des Cafres, France.
[5] Seismology Department, Institut de Physique du Globe de Paris, Sorbonne Paris Cité, Paris, France.

0148-0227/11/2010JB007636

Table 1. Main Characteristics of the Three Most Recent Basaltic Collapse Calderas

	Duration of the Whole Collapse Caldera Process	Number of Collapse Increments	Caldera Size (km^2)	Caldera Volume (km^3)	Maximum Depth (m)	Roof Aspect Ratio (Chamber Depth/Piston Diameter)
Piton de la Fournaise	~2 days	44	0.7	0.096[a]	320–340[b]	3.8
Miyakejima	~40 days	46[c]	2.3	0.6[c]	~450[c]	5.7
Fernandina	~12 days	~75[d]	7–8[d,e]	1–2[d,e]	300–350[d,e]	0.3[e]

[a]*Urai et al.* [2007].
[b]*Michon et al.* [2007].
[c]*Geshi et al.* [2002].
[d]*Filson et al.* [1973].
[e]*Simkin and Howard* [1970].

In basaltic setting, the time interval T between two successive collapse increments and the total duration of the whole collapse caldera process are key parameters that reveal the collapse dynamics [*Stix and Kobayashi*, 2008]. However, these parameters are significantly different from one caldera to another, and hence do not allow a direct comparison of the processes involved in each caldera formation. For instance, the total duration of the whole collapse caldera process varied from about 2 days at Piton de la Fournaise to 40 days at Miyakejima, without any correlation with the final volume of the caldera (Table 1) [*Kumagai et al.*, 2001; *Geshi et al.*, 2002; *Michon et al.*, 2007]. In addition, T gradually decreased at Piton de la Fournaise [*Michon et al.*, 2007; *Staudacher et al.*, 2009], remained constant then decreased at Fernandina [*Filson et al.*, 1973; *Stix and Kobayashi*, 2008], or fluctuated then increased at Miyakejima [*Ukawa et al.*, 2000; *Stix and Kobayashi*, 2008]. What is the common mechanics of caldera collapse behind the wide range of time scales observed?

[3] According to *Kumagai et al.* [2001], T may be expressed as a function of the frictional resistance along the ring faults (which is the subtraction of the static friction force F_S and the dynamic friction force F_D), the magma bulk modulus κ, the magma outflow rate α, the magma chamber volume V_0 and the cross-sectional area at the base of the piston-like subsiding rock column S:

$$T = \frac{2V_0(F_S - F_D)}{\kappa\alpha S} \tag{1}$$

Based on Fernandina and Miyakejima calderas, $F_S - F_D$ and κ have been considered of primary importance [*Simkin and Howard*, 1970; *Filson et al.*, 1973; *Kobayashi et al.*, 2003; *Stix and Kobayashi*, 2008] whereas variations in other parameters seemed to have little influence on the caldera collapse dynamics in basaltic setting [*Stix and Kobayashi*, 2008].

[4] The first goal of this paper is to re-investigate the role of the above parameters (α, V_0, $F_S - F_D$ and κ) in the evolution of T, taking advantage of the extensive database collected during the recent formation of Piton de la Fournaise caldera. This collapse was the first for which the link between the magma withdrawal and the collapse dynamics could be demonstrated. Indeed, the emission rate determined from direct observations and MODIS data [*Staudacher et al.*, 2009; *Coppola et al.*, 2009] was found to be temporally correlated with the incremental collapses of the rock column into the magma chamber. This suggests that the emission rate is proportional to the magma discharge rate from the reservoir [*Michon et al.*, 2007].

[5] A second important issue is the causal relationship between the collapsing column and the eruption/intrusion dynamics. Does the subsiding caldera block push the magma out of the magma chamber? Or does the collapse occur by magma underpressure in the reservoir? These questions have already been addressed in the case of silicic calderas [*Druitt and Sparks*, 1984; *Martí et al.*, 2000; *Folch et al.*, 2001; *Roche and Druitt*, 2001], yet whether the proposed explanations hold for basaltic calderas remains unverified. The pressure evolution in the magma chamber after each collapse increment may be expressed using the following relationship [*Kumagai et al.*, 2001]:

$$p_1 = p_0 + p - p't \tag{2}$$

p_0 and p_1 are the pressure in the magma chamber before and after a given collapse increment, respectively, p is the pressure increase due to the intrusion of the caldera block into the magma chamber, p' is the pressure decrease due to magma outflow and t is the time between two collapse increments, i.e., T. Pressures p and p' are given by

$$p = \kappa Sz/V_0 \text{ and } p' = \kappa\alpha/V_0 \tag{3}$$

where Sz is the volume of a caldera block intruded into the magma chamber, z corresponding to the vertical displacement during a given collapse increment. α is the rate of magma withdrawal from the magma chamber.

[6] According to equations (2) and (3), the condition for the magma to be pushed out of the magma chamber by a caldera collapse is that Sz be larger than the volume of magma αt withdrawn from the magma chamber before the collapse. This condition may be tested in the light of the 2007 collapse of Piton de la Fournaise caldera.

[7] To explore the different issues described above, we studied in detail the timing of caldera collapse relative to magma outflows, and correlated it to the deformation of the edifices during the collapse event. Using tiltmeter and/or seismic data recorded during each caldera collapse, we show that Piton de la Fournaise and Fernandina had strikingly similar collapse dynamics despite their scale differences, and that Miyakejima involved additional processes. Our study provides quantitative constraints on the relationship between the caldera dynamics, the edifice deformation

and the variations of the rate of magma withdrawal in basaltic setting.

2. Chronology of Caldera Formation and Related Seismicity

2.1. Piton de la Fournaise

[8] At Piton de la Fournaise, the eruption leading to caldera collapse initiated on 30 March 2007 with a dike injection yielding a short eruption 1 km east of the central cone. After an eruptive lull of 3 days, magma emission resumed on 2 April at a new eruptive fissure located 7 km east of the summit. The gap of eruptive activity contrasts with the continuous volcano-tectonic seismicity that developed below the summit of the edifice from 30 March and increased until 0200 GMT 5 April. On 1200 GMT 5 April the volcano experienced an increasing centripetal deflation until the first collapse at 2048 GMT. As pointed out by *Michon et al.* [2007], this event and the next six ones were followed by an increase of the tremor at the eruption site, suggesting a direct effect of the collapsing block on the magma chamber. Seismic and tiltmeter data showed the development of 44 collapse increments until 0009 GMT 8 April, the amplitude of which first slightly increased after the first largest event, then exponentially decreased to a minimum on 2233 GMT 6 April (Figure 1a). The collapse amplitude finally increased a bit until the last collapse. The time interval between the collapse increments varied from several hours to 30 min. The maximum tremor value recorded on 1200 GMT 6 April corresponds to a peak of magma emission, of at least 200 m^3s^{-1}, which progressively decreased until 0100 GMT 7 April [*Michon et al.*, 2007; *Staudacher et al.*, 2009]. The caldera collapse stopped on 8 April whereas the eruption continued at low level until 1 May. At the end of the event in May 2007, the summit caldera had a 0.7 km^2 surface, a maximum depth of 320–340 m and a total volume 96×10^{-3} km^3 (Table 1) [*Michon et al.*, 2007; *Urai et al.*, 2007]. Based upon an average piston diameter of 520 m and a magma chamber depth of about 2000 m [*Peltier et al.*, 2008], the roof aspect ratio (depth of the chamber roof dividing by its diameter) was 3.8.

2.2. Fernandina

[9] Due to its location in an uninhabited area and the very scarce monitoring network, limited to seismometers, the formation of the summit caldera at Fernandina is much less constrained than the two other natural cases. According to *Simkin and Howard* [1970], the volcanic activity started with a lateral eruption on 21 May 1968, the duration of which is not constrained due to a lack of later observations. Between 2 and 7 June, seismometers located at 140 km of Fernandina and in South and North Americas recorded an increasing amount of earthquakes until a probable volcanic explosion monitored by infrasonic stations [*Filson et al.*, 1973]. On 11 June, the dynamics of Fernandina changed drastically with the development of large summit phreatic then phreatomagmatic eruptions. Eruptions stopped on 12 June whereas the seismic activity increased throughout the day until a large earthquake (M_s = 5.1), which was interpreted as resulting from the first collapse of the roof of the magma chamber [*Simkin and Howard*, 1970; *Filson et al.*, 1973]. The subsequent seismicity was characterized by large events ($M_s \geq 5$) until 14 June. According to *Simkin and Howard* [1970], the regular time interval of 6 h observed until 14 June dropped to 3 h on 15 June, to 2 h on 17 June and to 60–90 min on 19 June. The end of the swarm was characterized by an increase of the interval between the largest events [*Simkin and Howard*, 1970]. The earthquake magnitude also decreased to M_s4.7–4.9 on 15 June and to $M_s <$ 4.5 between 17 and 20 June [*Filson et al.*, 1973; *Stix and Kobayashi*, 2008]. During this sequence, the first seismic events, i.e., between 12 and 14 June, accounted for nearly half of the total seismic energy released during the caldera collapse (Figure 1c) [*Simkin and Howard*, 1970]. The successive collapse increments led to the development of a 1–2 km^3 trap-door caldera with a maximum subsidence of the surface of 300–350 m [*Simkin and Howard*, 1970; *Filson et al.*, 1973] and a roof aspect ratio of ~0.3 [*Stix and Kobayashi*, 2008].

2.3. Miyakejima

[10] On 26 June 2000, a dike injection started from the 3- to 5-km-deep magma chamber of Miyakejima volcano [*Nishimura et al.*, 2001]. Magma rapidly migrated within the crust toward the WNW, feeding a small andesitic submarine eruption on 27 June. The intrusion-related seismic swarm was initially located below the summit and progressively propagated toward the WNW between −1 and −6 km depth [*Wright and Sakai*, 2004]. The dike injection triggered a sharp inflation of the southwestern half of the edifice [*Ueda et al.*, 2005; *Irwan et al.*, 2006], rapidly followed by a continuous centripetal deflation of the volcanic island [*Ito and Yoshioka*, 2002; *Murase et al.*, 2006]. From 4 July, earthquake activity below the summit was reactivated drawing a columnar swarm between the magma chamber and the sub-surface [*Geshi et al.*, 2002]. Initiation of the caldera collapse occurred on 8 July at the same time than a first summit phreatic eruption. Then the volcano underwent 46 collapse increments between 8 July and 18 August, i.e., about 40 days [*Ukawa et al.*, 2000; *Geshi et al.*, 2002]. 39 events out of the 46 collapses produced Very-Long-Period (VLP) seismic signals [*Kikuchi et al.*, 2001; *Kumagai et al.*, 2001]. The cumulative seismic energy released by these events and the rate of volumetric changes present a roughly linear increase interpreted as the result of a constant rate of magma withdrawal (Figure 1b) [*Kumagai et al.*, 2001; *Stix and Kobayashi*, 2008].

[11] By contrast with Piton de la Fournaise, the incremental subsidence at Miyakejima was coeval with 5 summit eruptions: two phreatic ones on 8 July and 10 August and three phreatomagmatic events on 14–15 July and 13 and 18 August [*Geshi and Oikawa*, 2008]. The composition change of the juvenile erupted products during the phreatomagmatic eruptions, from andesitic in July to basaltic in August, was interpreted as the result a deep magma injection between 15 July and 13 August [*Geshi and Oikawa*, 2008]. The summit eruptive activity and the distal seismic swarm persisted until mid-September 2000 [*Geshi et al.*, 2002; *Wright and Sakai*, 2004]. The 2000 eruption of Miyakejima led to the development of a ~450 m deep caldera with a diameter of 1.6 km and a volume of 0.6 km^3 [*Geshi et al.*, 2002]. Considering the piston diameter described by *Geshi et al.*

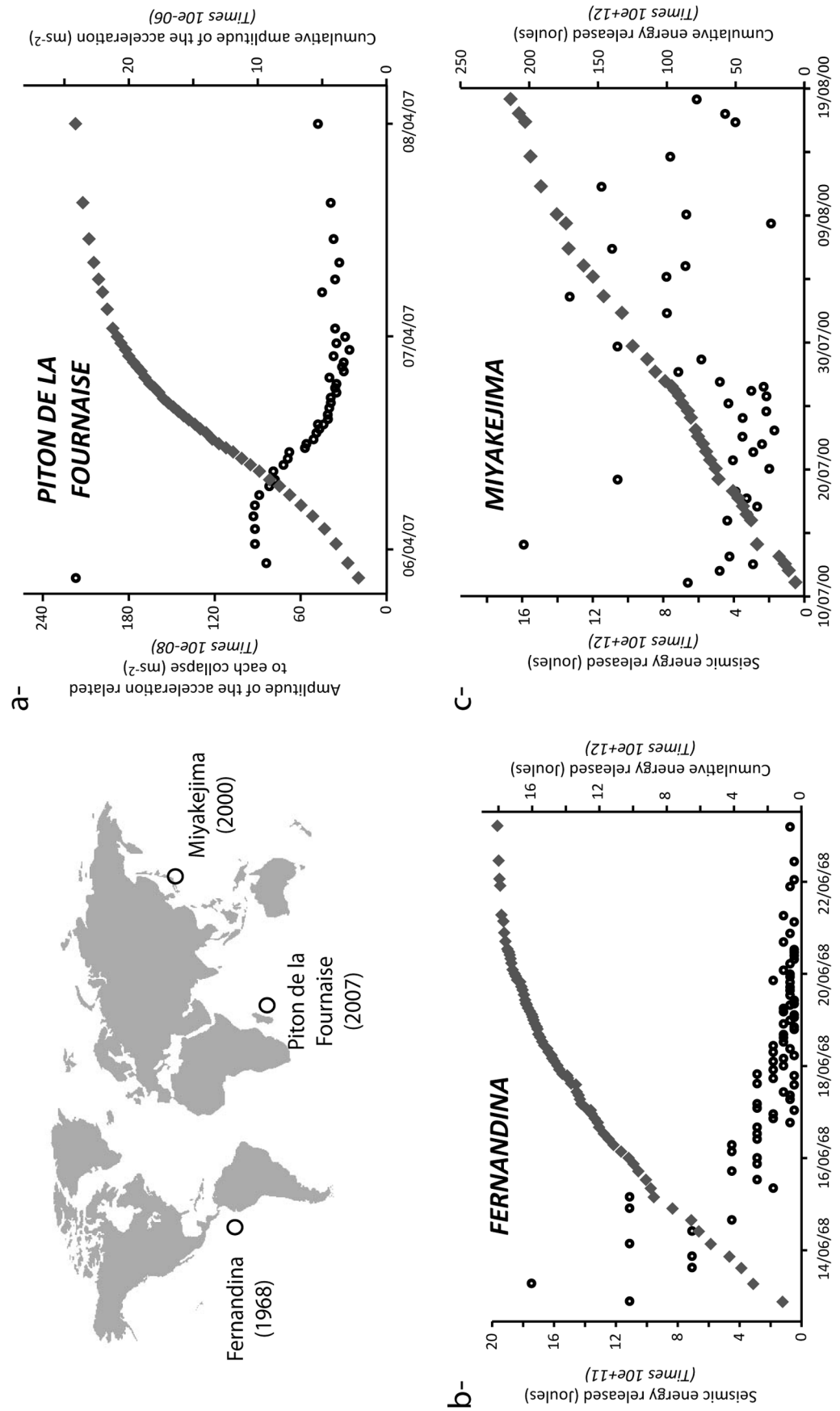

Figure 1. Individual (left-hand scale and open circles) and cumulative (right-hand scale and gray diamonds) amplitude of the collapse events at (a) Piton de la Fournaise, (b) Fernandina, and (c) Miyakejima. For Piton de la Fournaise, the amplitude is represented by the collapse-related acceleration determined from the N-S component of the RER broadband seismometer of the GEOSCOPE network located 8 km north of the summit. The seismometer is recording the ground velocity (seismic signal in count/m/s). The signal has been deconvoluted from the instrumental response and derived to obtain the acceleration in m s^{-2}. Data of Miyakejima are after *Stix and Kobayashi* [2008]. The released seismic energy during the collapse events of Fernandina was calculated as LogE = 1.96M + 2.05, where E is the energy in Joules, and M is the magnitude of the earthquake. Magnitudes are given by *Filson et al.* [1973].

[2002] and an average magma chamber depth of 4 km gives a roof aspect ratio of 5.7 (Table 1).

3. Timing of Caldera Collapse

[12] At Piton de la Fournaise and Miyakejima, the incremental collapses were coeval with sudden outward displacements of the edifice, producing successive tilt steps on tiltmeter data [*Ukawa et al.*, 2000; *Yamamoto et al.*, 2001; *Michon et al.*, 2007]. *T* was then considered as the duration between two successive tilt steps. A different approach has been developed for Fernandina. Based on the analysis of the number of events *N* of a given magnitude M_s, *Filson et al.* [1973] discriminated two different populations of seismic events related to the caldera collapse [see *Filson et al.*, 1973, Figure 12]. The largest events, $M_s > 4.5$, are interpreted as the result of the collapse of the caldera block whereas the smaller earthquakes would represent secondary adjustments and landslides. However, there is an ambiguity in the work of *Filson et al.* [1973] because the authors proposed the occurrence of 75 collapse increments whereas only 43 seismic events have a magnitude larger than 4.5. Given this disagreement and the uncertainty on the origin of the earthquakes characterized by a magnitude close to the transition between the two groups, i.e., incremental collapse or readjustments, we chose two thresholds of earthquake magnitude to define *T*: taking earthquakes magnitude greater than 4.3 yields a set of 77 seismic events consistent with the number of collapses estimated by *Filson et al.* [1973]. Alternatively, Piton de la Fournaise data suggest that $M_s4.4$ is a better threshold to define caldera incremental collapses (see below). Applied to Fernandina, this threshold restricts the data set to 59 events.

[13] After reprocessing, whatever the method used, Piton de la Fournaise, Fernandina and Miyakejima present a first-order roughly similar evolution of *T*. *T* first decreases until a minimum level and then increases to its maximum value (Figure 2a). At a second order, two different evolutions of *T* can be identified for Piton de la Fournaise and Fernandina on the one hand, and Miyakejima on the other hand (Figures 2b and 2c). Despite differences in the total number of collapse increments, *T* variations for Piton de la Fournaise and Fernandina draw strikingly similar patterns: a decrease during 30–33% of the collapse increment total number, followed by a relatively constant level between 30 and 33% and 86–91% of the collapse increment total number, before a sharp increase until the last collapse increment (Figure 2b). The similar values of T_{norm}, the normalized *T* with respect to its longest value T_{max}, for both volcanoes confirm the almost identical collapse dynamics of Piton de la Fournaise and Fernandina (Figure 2c). T_{norm} decreases from about 0.2–0.3 for the initial collapses to constant level at around 0.1, before the rapid final increase. Note that the similar collapse dynamics of Piton de la Fournaise and Fernandina, for earthquakes having $M_s > 4.4$ suggests that the whole caldera collapse of Fernandina results from about 59 collapse increments instead of 75.

[14] The collapse dynamics of Miyakejima shows many differences with those of Fernandina and Piton de la Fournaise. The distribution of *T* during the caldera collapse of Miyakejima is much more scattered throughout the event. *T* increases early in the collapse caldera process, i.e., for $n = 0.6$ instead of $n = 0.85$–0.9 at Piton de la Fournaise and Fernandina (Figure 2c). *T* finally decreases before the end of the caldera collapse whereas it simply increases on the two other volcanoes. It is worth noting that the final *T* decrease at Miyakejima was coeval with summit eruptions, which lack at Piton de la Fournaise and Fernandina during the same final period.

[15] We consider next the amplitude of collapse increments through time for the three studied calderas and the edifice deformation of Piton de la Fournaise and Miyakejima during their caldera collapse, in order to determine a collapse-related evolution as complete as possible for each volcano.

4. Amplitude of the Collapse Increments and Magma Outflow Rates Through Time

[16] A posteriori quantification of the caldera block downward displacement during each collapse increment may be performed if the total amount of vertical collapse and the relative amplitude of each collapse are known. The caldera collapse of Fernandina triggered a downward displacement of 300–350 m of the initial caldera floor [*Simkin and Howard*, 1970; *Filson et al.*, 1973]. For Miyakejima, *Geshi* [2009] inferred a total collapse of about 1600 m, i.e., the volume of the caldera (6×10^8 m^3) divided by the observed surface of the piston (384×10^3 m^2). With the same approach, we determined a total collapse of about 450 m for Piton de la Fournaise; the ratio between a caldera volume of 96×10^6 m^3 [*Urai et al.*, 2007] and the surface of the piston of 212×10^3 m^2 deduced from orthorectified images of the caldera.

[17] Assuming that (1) the acceleration amplitude or the seismic energy released by each collapse increment at Piton de la Fournaise and Fernandina (Figure 1) is proportional to the amount of piston downward displacement and (2) the cumulative acceleration amplitude or the cumulative seismic energy released accounts for the vertical total collapse (450 m at Piton de la Fournaise and a mean value of 325 m for Fernandina), we calculated the downward displacement associated with each collapse increment and the subsequent volumetric changes in the magma chamber (Figure 3a). It is worth noting that the displacements inferred for Fernandina present relatively large (yet impossible to quantify) uncertainties due to the scattered and distant characteristics of the seismic network.

[18] For Miyakejima, volumetric changes have been already determined from VLP signals [*Kumagai et al.*, 2001]. However, since only 39 out of the 46 collapses triggered VLP signals, we preferentially used tiltmeter data of *Yamamoto et al.* [2001] to infer the vertical collapse amplitude and subsequently the volume changes. The remarkably parallel evolution of the tilt step amplitude, the volume changes [*Kumagai et al.*, 2001] and the released seismic energy [*Kikuchi et al.*, 2001] clearly indicates that tilt steps are as appropriate as VLP signals for estimating the relative amplitude of collapses (Figure 4). Most importantly, as tilt data recorded the 46 collapse events, they provide a complete picture of the evolution of the collapse amplitude throughout the caldera development.

[19] Our results on the downward displacements show that each caldera experienced maximum vertical displace-

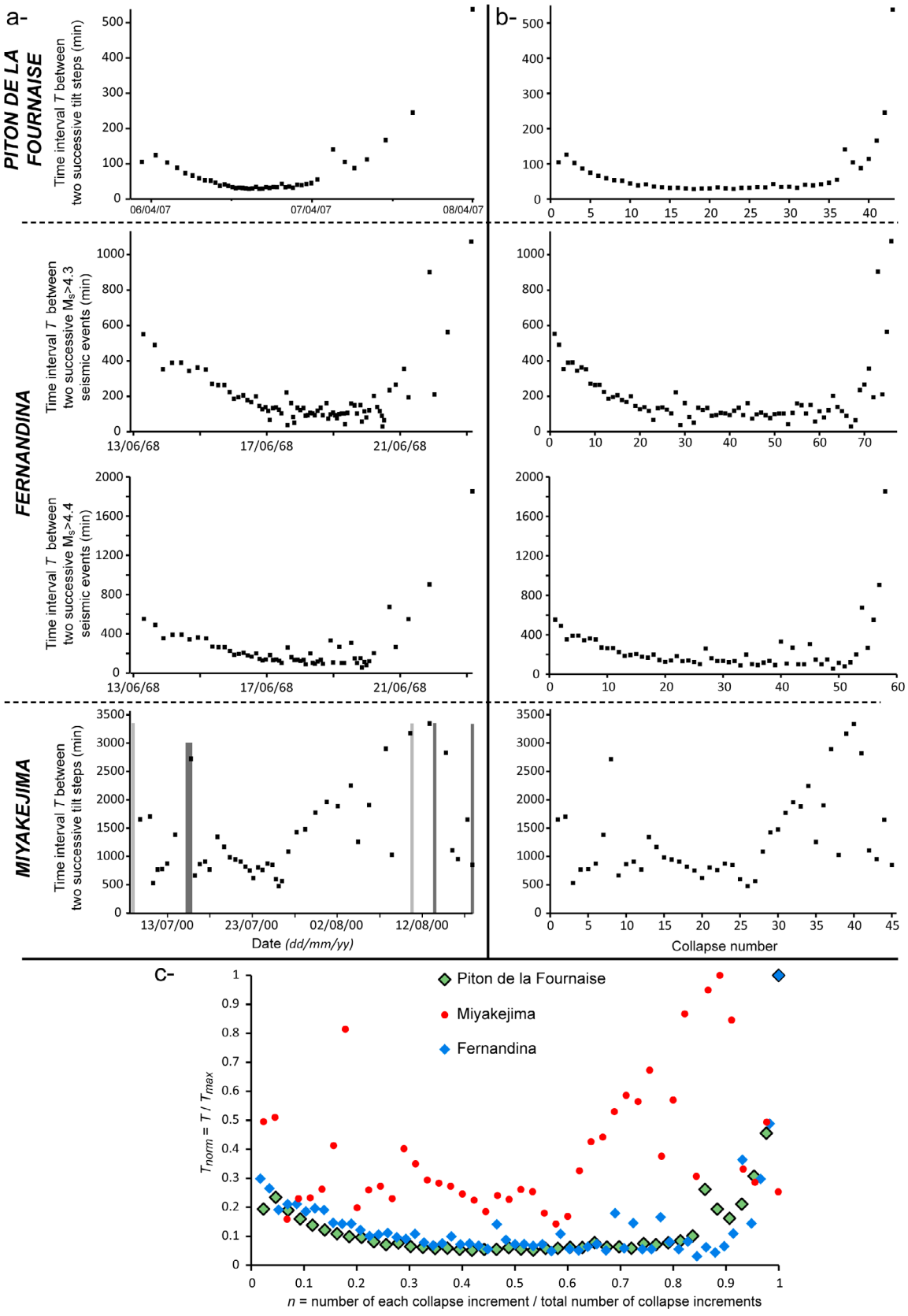

Figure 2. (a) Evolution of T during the whole collapse caldera processes at Piton de la Fournaise, Fernandina, and Miyakejima. (b) Individual time interval with respect to the collapse total number. (c) Normalized T ($T_{norm} = T / T_{max}$) and collapse number (n = number of each collapse increment / total number of collapse increment).

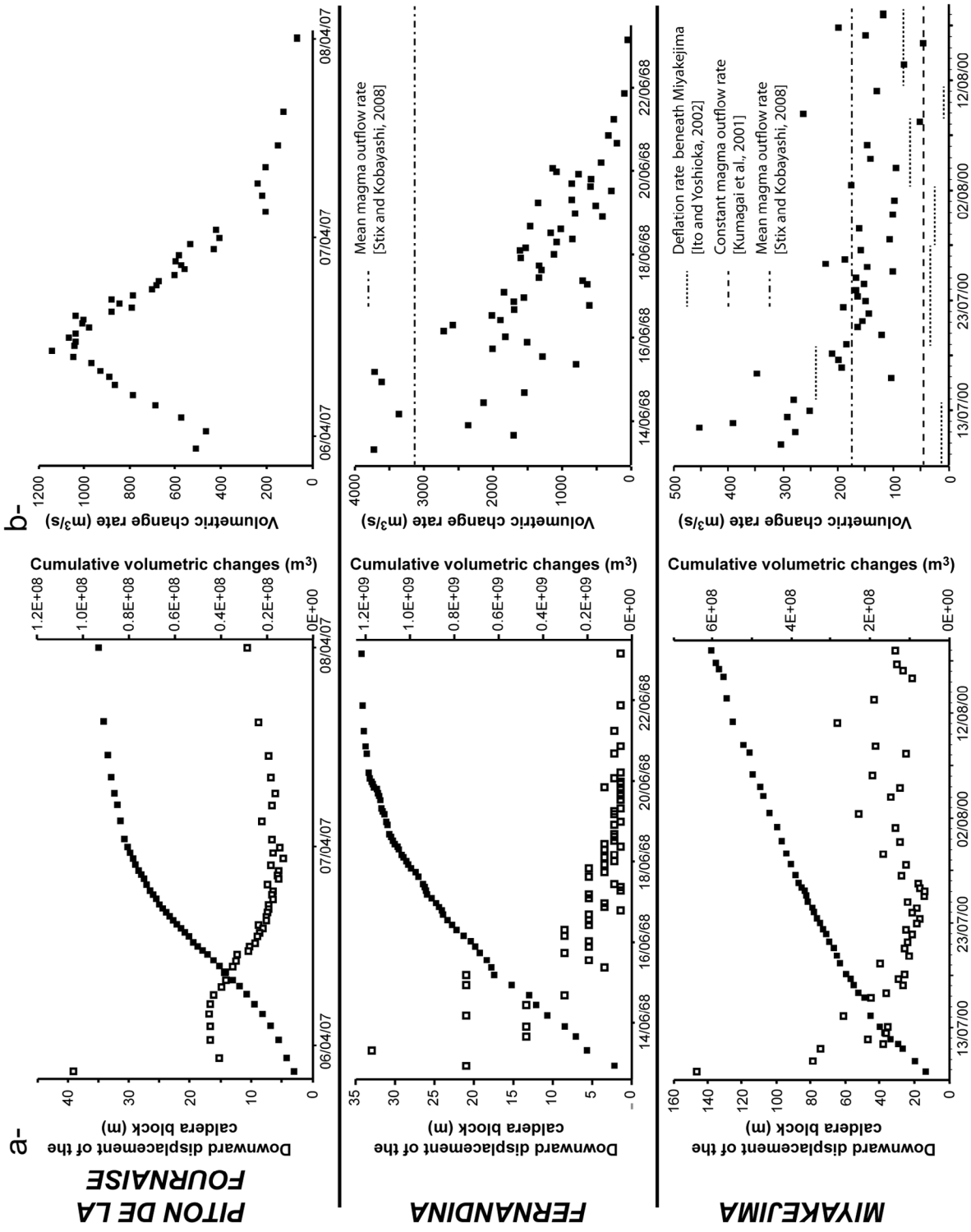

Figure 3. (a) Downward displacements during each collapse increments and the resulting cumulative volumetric changes in the magma chamber. (b) Volumetric change rates inferred from the volumetric changes and the time interval between two collapse increments. See text for explanation.

ments during their first collapse increments, i.e., 39 m, 32 m and 147 m at Piton de la Fournaise, Fernandina and Miyakejima, respectively (Figure 3a). For Miyakejima, this value outstandingly agrees with observations, which indicate the development of a 140-m-deep caldera after the first collapse increment [*Geshi et al.*, 2002]. In the case of Fernandina, our result is significantly larger than the 8–18 m of collapse proposed by *Stix and Kobayashi* [2008]. Next the downward displacement amplitudes rapidly decreased except at Piton de la Fournaise where they first remained at a relatively constant level, around 15–17 m, during the 6 subsequent collapse increments and next lowered. For Miyakejima and Piton de la Fournaise, values reached a minimum (~10% of the maximum displacement) about halfway through the whole collapse events, whereas they continuously decreased at Fernandina until the end of the collapse caldera process. After the low level, downward displacements slightly and progressively increased until 11 m at Piton de la Fournaise, while they rapidly doubled at Miyakejima from 28 July and then remained at a strongly fluctuating high level (from 20 m to 65 m) until the end of the caldera development (Figure 3a). The occurrence of relatively large collapses during this last phase triggered a linear increase of the cumulative volumetric changes, i.e., the cumulated volume of caldera block intruded into the magma chamber, as already mentioned by *Kumagai et al.* [2001]. This evolution contrasts with those of Piton de la Fournaise and Fernandina where the cumulative volumetric changes are characterized by an attenuation of the augmentation during the second half of the collapse caldera process.

[20] Dividing the volumetric change related to each collapse increment by the time interval T, we quantified the volumetric change rate, usually interpreted as similar to the magma outflow rate [*Kumagai et al.*, 2001; *Stix and Kobayashi*, 2008], throughout the collapse processes. Figure 3b first reveals that the volumetric change rates notably differed for the three studied calderas. Maximum rates of 1133 m^3 s^{-1}, 3724 m^3 s^{-1} and 454 m^3 s^{-1} have been determined for Piton de la Fournaise, Fernandina and Miyakejima, respectively. Figure 3b also shows distinct evolutions of the volumetric change rates for each caldera. At Piton de la Fournaise, the volumetric change rate increased during the first 11 collapse increments, from 460 m^3 s^{-1} to 1133 m^3 s^{-1}, then remained stable around 1000 m^3 s^{-1} during eight collapse increments, and underwent a first rapid then slow decrease until 68 m^3 s^{-1} at the end of the collapse caldera process.

[21] For Fernandina, the volumetric change rate strongly varied between 796 m^3 s^{-1} and 3724 m^3 s^{-1}, from 12 June (the onset of collapse) to 16 June. Such variations may reflect real changes in the caldera dynamics. However, it must be kept in mind that volumetric change rates depend primarily on the downward displacement amplitudes, on which there are large uncertainties, as explained above. From 16 June, the volumetric change rates decreased from about 2000 m^3 s^{-1} to 47 m^3 s^{-1} at the end of the collapse process, in a way roughly similar to the final decrease observed for Piton de la Fournaise. Integration of our volumetric change rates for the whole caldera collapse suggests a mean value of 1341 m^3 s^{-1}, which significantly differs from the 3000–3400 m^3 s^{-1} estimate of *Stix and Kobayashi* [2008]. However, this difference is mostly explained by a shorter total collapse duration, 182 h in their work and 242 h in ours (from 2221 GMT 12 June to 0343 GMT 23 June), and a caldera volume of 2.2×10^9 m^3, larger than the previous volume estimates, between 1×10^9 m^3 and 2×10^9 m^3 [*Simkin and Howard*, 1970; *Filson et al.*, 1973].

[22] By contrast with Piton de la Fournaise and Fernandina, Miyakejima experienced a twofold average evolution of the volumetric change rate (Figure 3b). Between the collapse onset on 8 and 21 July, the volumetric change rates decreased from 454 m^3 s^{-1} to ~150 m^3 s^{-1}. Afterward, they fluctuated between 47 m^3 s^{-1} and 264 m^3 s^{-1}, at an almost constant mean volumetric change rate of ~140 m^3 s^{-1}. These values and their variations strongly differ from those proposed by *Ito and Yoshioka* [2002] and *Kumagai et al.* [2001] (Figure 3b). However, their integration during the whole caldera collapse gives a mean volumetric change rate of 155 m^3 s^{-1}, which is almost similar to the 170 m^3 s^{-1} proposed by *Stix and Kobayashi* [2008] for the mean magma outflow rate.

5. Edifice Deformation During Caldera Collapse

[23] Two main results have already been reported concerning the deformation of Piton de la Fournaise and Miyakejima during their caldera collapse. First, these events were coeval with an overall centripetal deflation of both edifices [*Ito and Yoshioka*, 2002; *Murase et al.*, 2006; *Michon et al.*, 2007, 2009; *Staudacher et al.*, 2009]. Second, the volcano experienced successive phases of progressive inward subsidence ended by sudden outward inflation while the caldera roof was collapsing in the magma chamber [*Ukawa et al.*, 2000; *Michon et al.*, 2007]. We combine here GPS, tiltmeter and seismic data in order to refine the edifice deformation during both caldera collapses.

5.1. Piton de la Fournaise

[24] The deformation of Piton de la Fournaise has been monitored by the geodetic network of the Piton de la Fournaise Volcano Observatory. Data recorded by the TCRI tiltmeter station show the occurrence of 44 tilt steps between 2048 GMT 5 April and 0009 GMT 8 April (Figure 5a). Due to local site effects, the largest deformation amplitudes are recorded on the TCRI tangential component. An interesting aspect revealed by tilt and GPS data is a long-term edifice deformation. TCRI station shows a decreasing trend of the initial slope values after the first 9 collapse increments followed by an increase until the last collapse event (Figure 5a). GPS data indicate that the first and second trends represent periods of outward and inward displacements of the edifice, respectively. These variations suggest that besides the elastic response of the edifice, the volcano experienced a twofold long-term deformation corresponding to the edifice inflation followed by its deflation (Figure 5b).

[25] Tilt data are also used to determine the critical amount of deformation experienced by the edifice before the collapse of the rock column. The tangential component of TCRI reveals a slope variation of 28 μrad before the first collapse increment. Once the collapse initiated the amount of slope variation decreased from about 9 μrad after the first collapse increment to a low level around 3 μrad, between 1400 GMT 6 April and 0100 GMT 7 April (Figure 5c). Then, failure occurred for increasing amount of deformation

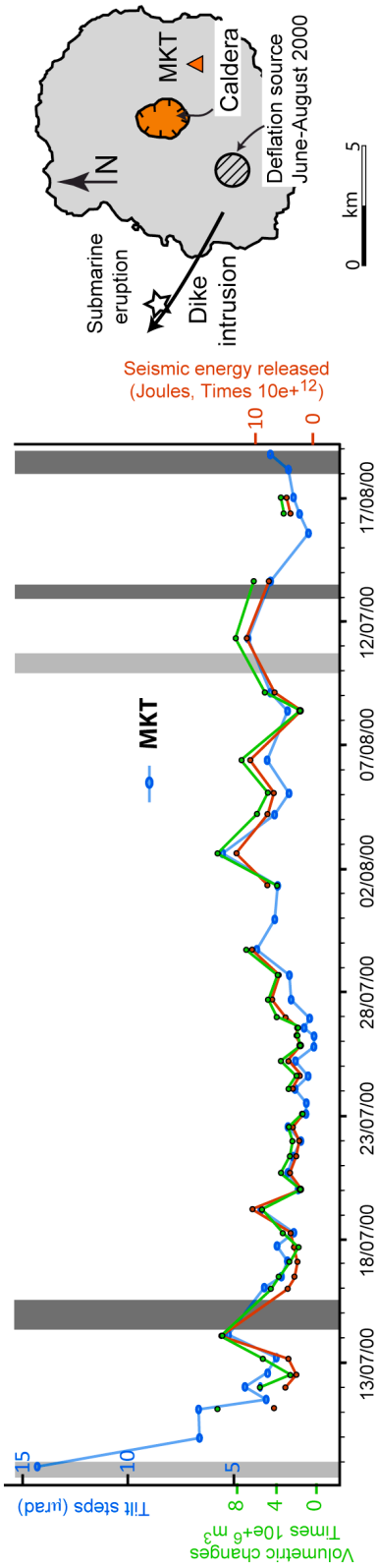

Figure 4. Evolution of the tilt step amplitude recorded at the MKT station [after *Yamamoto et al.*, 2001] and of the volumetric changes [after *Kumagai et al.*, 2001] and the seismic energy released inferred from the 39 VLP events [after *Kikuchi et al.*, 2001] during the caldera collapse of Miyakejima.

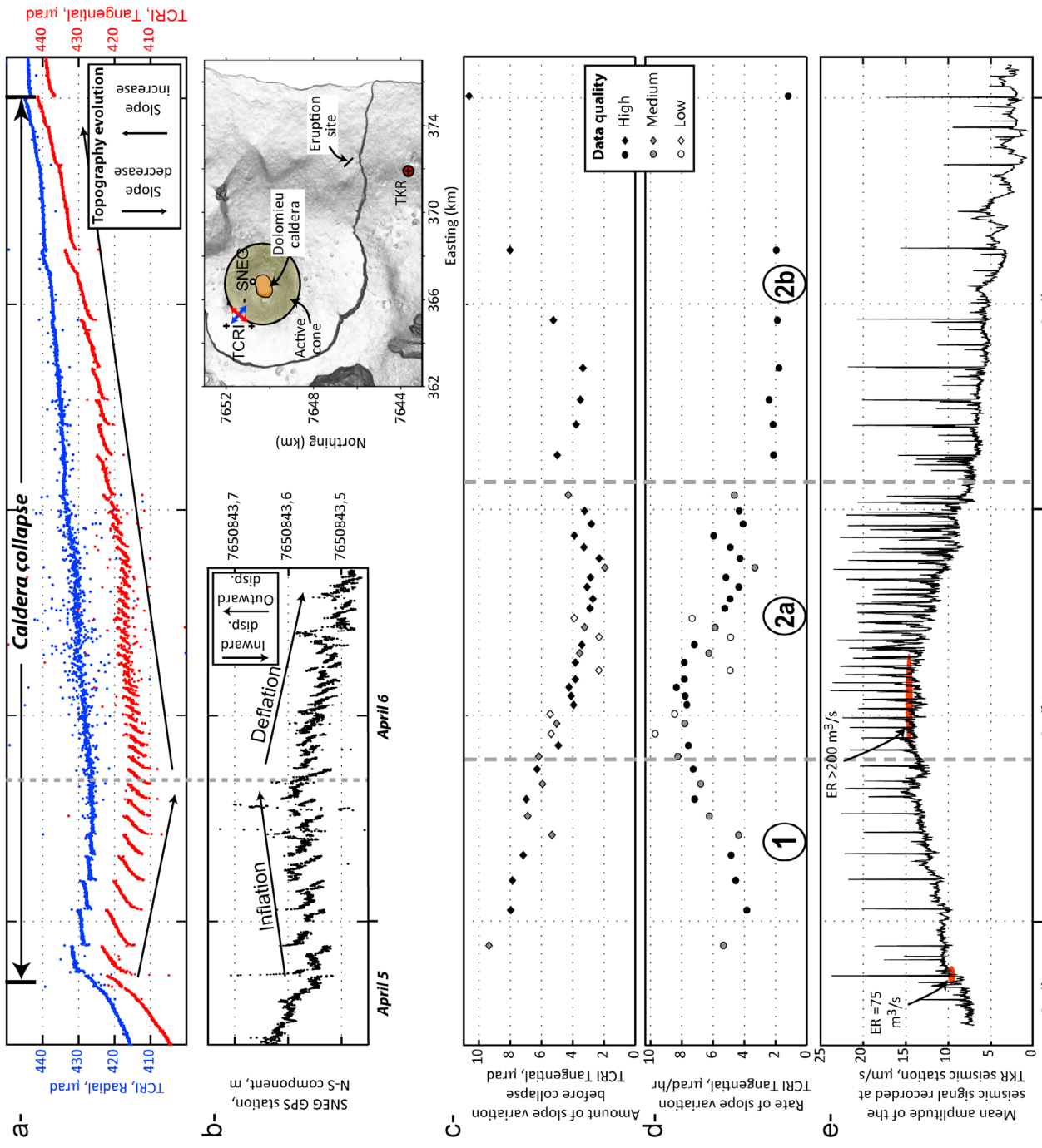
a-
TCRI, Radial, µrad
TCRI, Tangential, µrad
Caldera collapse
Topography evolution
Slope decrease
Slope increase
b-
SNEG GPS station, N-S component, m
Inflation
Deflation
Inward disp.
Outward disp.
April 5
April 6
Northing (km)
Easting (km)
SNEG
TCRI
Dolomieu caldera
Active cone
Eruption site
TKR
c-
Amount of slope variation before collapse TCRI Tangential, µrad
Data quality
High
Medium
Low
d-
Rate of slope variation TCRI Tangential, µrad/hr
1
2a
2b
e-
Mean amplitude of the seismic signal recorded at TKR seismic station, µm/s
ER =75 m3/s
ER >200 m3/s
April 5
April 6
April 7

Figure 5

up to a maximum value of 10.5 μrad at the end of the caldera collapse.

[26] Dividing the amount of slope variation for each collapse cycle by its duration, *T*, enables assessments of the rate of deformation during the successive collapse cycles (Figure 5d). Data indicate that after the first collapse cycle, the rate of edifice deformation increased up to an average value of about 8 μrad/h between 1100 and 1300 GMT 6 April. After that, the rate of deformation lowered, first rapidly until 0100 GMT 7 April, then slowly. This evolution is remarkably similar to that of the mean amplitude of the seismic signal recorded by the TKR seismic station, close to the eruption site (Figure 5e). It has been shown that (1) the seismic amplitude and the emission rate had parallel evolutions [*Coppola et al.*, 2009; *Staudacher et al.*, 2009] and (2) the seismic amplitude was strongly influenced by the collapse of the rock column into the magma chamber [*Michon et al.*, 2007]. Thus, we propose that the rate of edifice deformation gives qualitative insights into that of magma outflow from the magma reservoir.

[27] Two phases were discriminated from the variations of both the rate of edifice deformation and the seismic amplitude (Figure 5). Phase 1 is characterized by an increasing rate of deformation concomitant with the emission rate and by a decrease of the amount of deformation before failure. Phase 2 starts when the slope variation rate ceases to increase. It is subdivided in two periods 2a and 2b, characterized by a rapid and slow decrease of both parameters, respectively. Note that phase 2b starts when the critical amount of deformation yielding to failure along the ring faults increases. These phases 1, 2a and 2b are strictly contemporaneous with the increase, rapid decrease and slow decrease of the volumetric change rates (Figure 3b).

5.2. Miyakejima

[28] The caldera collapse of Miyakejima was preceded by a period of deflation, triggered by the 26 June northwestward dike intrusion [*Ito and Yoshioka*, 2002]. Magma withdrawal from the 3- to 5-km-deep magma chamber [*Nishimura et al.*, 2001; *Murase et al.*, 2006] led to the destabilization of the rock column on 8 July, and subsequently to its incremental collapses until 18 August (Figure 6a). As in the case of Piton de la Fournaise, tiltmeter data allowed the determination of the amount of deformation preceding each collapse event. Data inferred from the N-S component of the MKK tiltmeter reveal a slope variation of ~82 μrad before the first collapse increment. The amount of slope variation drastically decreased after this first event, drawing a decreasing trend between 7 μrad to 1.5 μrad until 24 July (Figure 6b). Slope variations next tend to increase up to ~8 μrad on 8, 11 and 13 August, before a final decrease coeval with the phreatomagmatic summit eruptions on 13 and 18 August.

[29] Integration of both the time interval and the amount of slope variation suggests that the deformation of Miyakejima was characterized by three successive periods (Figure 6c). The rate of deformation first increased between the onset of the caldera collapse and 13 July. Although much shorter, this augmentation is relatively similar to that of phase 1 at Piton de la Fournaise. Then, the deformation rate presents a rapid decrease between 13 and 24 July, comparable to phase 2a at Piton de la Fournaise. Finally, the rate of deformation remained almost constant until the end of the caldera collapse. This period, which differs from phase 2b observed at Piton de la Fournaise by a lack of decrease, is labeled phase 3.

[30] GPS data from the NIED Miyakejima observation network [*Ukawa et al.*, 2000] are used to determine the edifice large-scale deformation during the caldera collapse. Variations of the baseline's length between two couples of GPS stations show that once the collapse initiated on 8 July, baseline's lengths ceased to decrease and instead increased until 13 July (phase I_1 in Figure 6d). The periods of decreasing then increasing baseline lengths correspond to phases of inward deflation and outward uplift, respectively [*Murase et al.*, 2006]. The inflation phase was followed by a period of deflation lasting 7 days, between 13 and 20 July (period D_1 in Figure 6d). Deflation came to a halt on 20 July. At that time, the slight increase of the baseline lengths reveals the occurrence of a 3-days-long inflation phase, I_2, until 23 July (period I_2 in Figure 6d). Afterward, the edifice deflated again even after the end of the collapse caldera process.

6. Discussion

6.1. Amount of Magma Evacuated Before Collapse

[31] From a hazard point of view, the critical volume fraction of magma evacuated f_{crit} before caldera collapse is a parameter of primary importance to evaluate if a given eruption will trigger the collapse of the magma chamber roof. Analysis of past eruptions in silicic setting and of analog models reveals that the greater the caldera roof aspect ratio *R*, the larger f_{crit} [*Roche and Druitt*, 2001; *Geyer et al.*, 2006]. f_{crit} evolves from 7% to 94% for *R* ranging between 0.2 and 3.2, respectively [*Aramaki*, 1984; *Druitt and Sparks*, 1984; *Pyle*, 1990; *Pallister et al.*, 1996; *Cioni et al.*, 1999; *Wallace et al.*, 1999; *Gardner and Tait*, 2000]. Assuming, as many authors did [e.g., *Druitt and Bacon*, 1989; *Martí et al.*, 2000; *Roche and Druitt*, 2001], an almost entire emptying of the magma chamber at the end of the collapse caldera process, we determined upper bounds of f_{crit} for the three studied caldera collapses as the ratio between the volume of piston intruded in the magma chamber during the first collapse increment and the caldera total volume. This

Figure 5. Deformation of Piton de la Fournaise during the 2007 caldera collapse. (a) Tilt changes recorded by the TCRI tiltmeter stations between 1600 GMT 5 April and 0200 GMT 8 April. Radial and tangential tilts are parallel and perpendicular to the slope, respectively. (b) Displacement of the northern rim of the caldera monitored by the SNEG GPS station [after *Staudacher et al.*, 2009]. (c) Amount and (d) rate of slope variation inferred from the tangential component of the TCRI tiltmeter. (e) Mean amplitude per minute of the seismic signal recorded by the TKR seismic station. ER, Emission rate proposed by *Coppola et al.* [2009] and *Staudacher et al.* [2009]. 1, 2a and 2b account for the successive phases identified from both the rate of slope variation and the mean amplitude of the seismic signal.

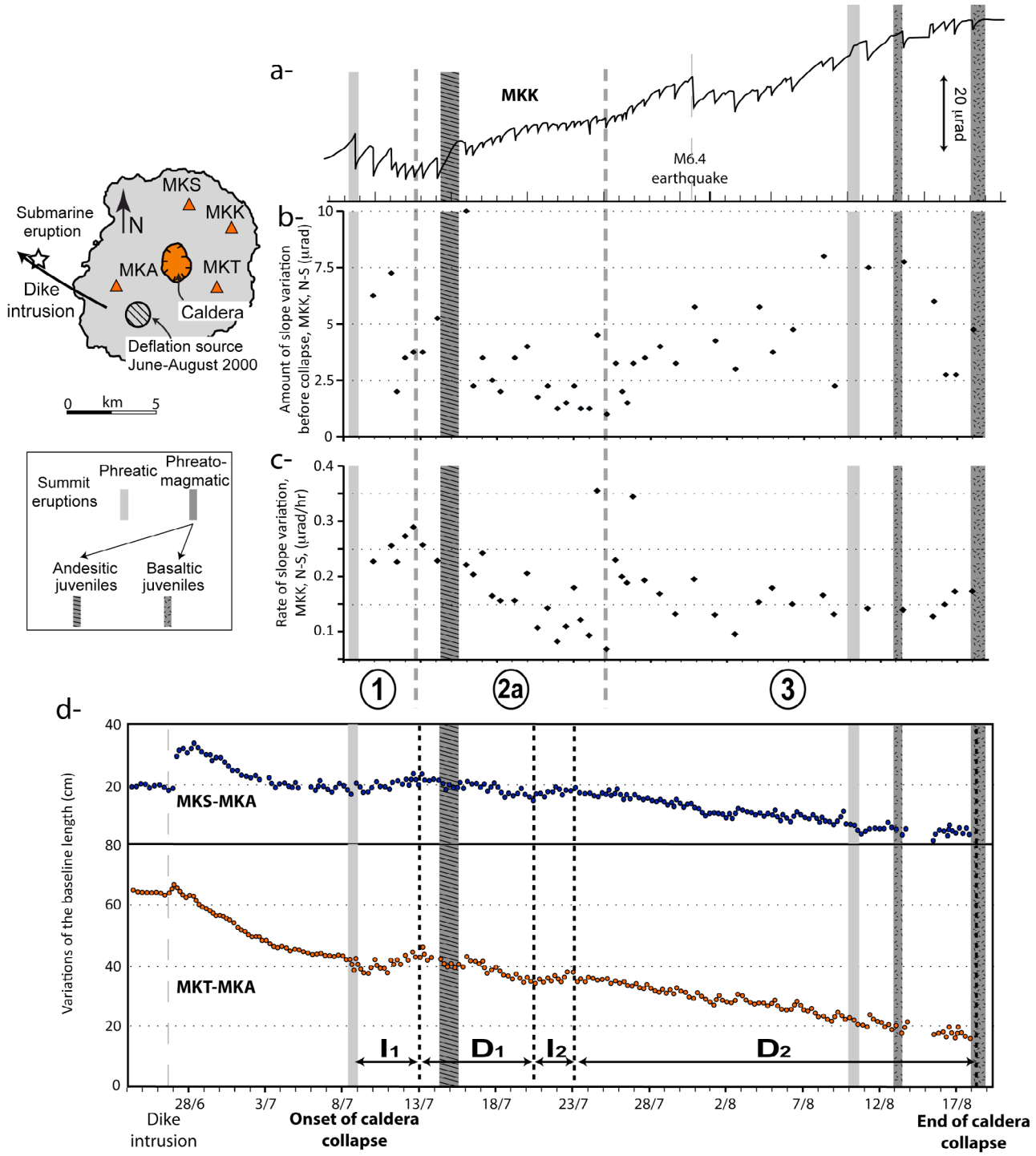

Figure 6. Deformation of Miyakejima during the 2000 caldera collapse. (a) Tilt changes along the N-S component of the MKK tiltmeter station [after *Ukawa et al.*, 2000]. (b) Amount and (c) rate of slope variation inferred from the radial component of the MKK tiltmeter. (d) Baseline lengths between the MKS-MKA and MKT-MKA GPS stations [after *Ukawa et al.*, 2000]. I_1 and I_2 correspond to the first and second periods of inflation. D_1 and D_2 represent the first and second periods of deflation. 1, 2a and 3 account for the successive phases identified from the rate of slope variation. The deflation source is located SW of the summit at 4–5 km below sea level [*Nishimura et al.*, 2001; *Murase et al.*, 2006].

yields f_{crit} of 8.2%, 6.4% and 9.4% for Piton de la Fournaise, Fernandina and Miyakejima, respectively. Note that these values would be smaller if magma is left in the magma chamber following caldera collapse. The results confirm the relationship between R and f_{crit}. However, our values are much smaller than theoretical ones inferred from analog models [*Geyer et al.*, 2006], i.e., 73.4%, 16.5% and 82.5% for Piton de la Fournaise (R = 3.8), Fernandina (R = 0.3) and Miyakejima (R = 5.7), respectively. Such a difference may have two possible causes. The first possibility is the pre-existence of ring faults resulting from earlier caldera collapses and along which fluids of the hydrothermal system migrate and reduce the edifice strength. Thus, rupture of the caldera roof occurs for values of underpressure lower than expected from isotropic analog models. The second possibility, as shown by *Martí et al.* [2000], is that f_{crit} depends essentially on the edifice strength, the magma chamber depth and the magma gas content. Caldera collapse should occur for f_{crit} of a few percent up to 40% for deep gas-poor and shallow gas-rich magma chambers, respectively. Thus, we interpret the basaltic to basaltic-andesitic magma composition [*Nakada et al.*, 2005; *Villemant et al.*, 2009] and/or a low edifice strength as the possible causes of the early caldera collapse of Piton de la Fournaise, Fernandina and Miyakejima.

6.2. Collapse-Related Edifice Inflation

[32] The causal relationship between magma withdrawal from a sub-surface reservoir and the edifice centripetal deflation is well known [e.g., *Wilson*, 1935; *Walsh and Decker*, 1971; *Dvorak*, 1992; *Roche et al.*, 2000; *Geyer et al.* 2006]. GPS and tiltmeter data recorded at Miyakejima [*Ukawa et al.*, 2000; *Yamamoto et al.*, 2001] and Piton de la Fournaise [*Michon et al.*, 2007; *Staudacher et al.*, 2009] during the summit caldera collapses reveal that despite the overall prominent deflation, the edifices also experienced pulses of outward inflation while the caldera block was collapsing. Edifice inflation occurred on both volcanoes after the first collapse increment (Figure 7). A second inflation phase took place at Miyakejima between 20 and 23 July, while the collapse increment amplitude had drastically decreased (Figure 7c).

[33] Edifice inflations are in general related either to upward magma migrations [e.g., *Lénat et al.*, 1989] or to pressure increase in the magma chamber [e.g., *Dieterich and Decker*, 1975; *Delaney and McTigue*, 1994] and/or in the hydrothermal system [e.g., *Bonafede*, 1991; *Dzurisin et al.*, 1994]. The edifice inflation recorded at Miyakejima after the initiation of the caldera collapse has been recently interpreted as resulting from an upward magma migration having led to the 14–15 July phreatomagmatic summit eruption [*Murase et al.*, 2006]. Yet, GPS data [*Ukawa et al.*, 2000] indicate that the edifice was already deflating since 12 July, 2 days before the eruption (Figure 6d). Thus, deflation predated eruption, which is not consistent with a magma progressive upward migration between 8 and 14 July.

[34] According to equation (2), a given collapse increment may produce overpressure in the magma chamber if the volume of piston intruded into the magma chamber exceeds that of magma withdrawn from the magma reservoir before the collapse [*Kumagai et al.*, 2001]. For Piton de la Fournaise and Miyakejima, the incremental edifice inflation recorded after the onset of caldera collapse was coeval with the piston largest vertical displacements, i.e., the largest volumes inserted into the magma chamber (Figure 7c). Inflation was also contemporaneous with a period of increasing slope variation rates for both volcanoes (Figure 7). We also showed for Piton de la Fournaise that changes of the slope variation rates were linked to modifications of the magma outflow rates (Figures 5 and 7). We therefore propose that the first large collapse increments related to the caldera collapse of Piton de la Fournaise and Miyakejima triggered overpressure in the magma chamber that caused edifice inflation and the increase of magma evacuation rates. *Martí et al.* [2000] already pointed out the pressure increase in the magma chamber after the beginning of the caldera collapse and the related discharge rate augmentation. However, the authors assumed that without any intracaldera deposit magma pressure increases in the reservoir up to a lithostatic maximum bound only. Here, the incremental edifice inflation recorded at Piton de la Fournaise and Miyakejima during the first collapse increments suggests that the pressure in the magma chamber exceeded the lithostatic bound. Knowing that the load of the piston did not increase during the caldera collapse (no syn-eruptive deposit in the caldera), we propose that the incremental over-lithostatic could result from the conversion of the kinetic energy related to the piston displacement during the largest collapses, as mentioned in the laws of energy and momentum conservation.

[35] Whatever the cause of the pressure increase, the piston forcefully pushed magma out of the reservoir during the first 10 and 6 collapse increments at Piton de la Fournaise and Miyakejima, respectively. Then, the slope variation rates stopped increasing and the edifices started deflating. Edifice deflation, which was coeval with a rapid decrease of the rate of magma withdrawal suggests that the effect of the caldera block on the magma chamber vanished with time. This twofold evolution, i.e., increase then decrease of the magma outflow rate, is similar to that proposed for caldera collapse in silicic setting where the eruption rate first increases due to the load of the piston and next decreases when most of the volatiles are ejected from the magma reservoir [*Folch and Martí.*, 2009].

[36] *Troise et al.* [2003] showed that inflation tends to facilitate normal slip along the ring faults. The edifice expansion due to the collapsing rock column therefore corresponds to a process that could further enhance the collapse of the caldera block into the magma chamber. Applied to silicic calderas, which are supposed to be also bounded by vertical an/or outward dipping faults [*Roche et al.*, 2000], expansion is an additional mechanism that may promote magma migration along the ring faults by opening them.

[37] GPS data show that Miyakejima experienced a second inflation phase between 20 and 23 July during a period of minimum collapse amplitude. A causal relationship between the amount of vertical collapse and the inflation is therefore unlikely. Furthermore, the phases of edifice inflation did not predate summit eruptions, making the hypothesis of magma migration from the magma chamber to the surface doubtful. According to *Ito and Yoshioka* [2002], the intrusion dynamics changed between 20 and 28 July, a period during which the rate of dike intrusion was maximum and sub-crustal magma reservoirs started to feed the dike. We consequently propose that edifice inflation I_2 (Figure 6d)

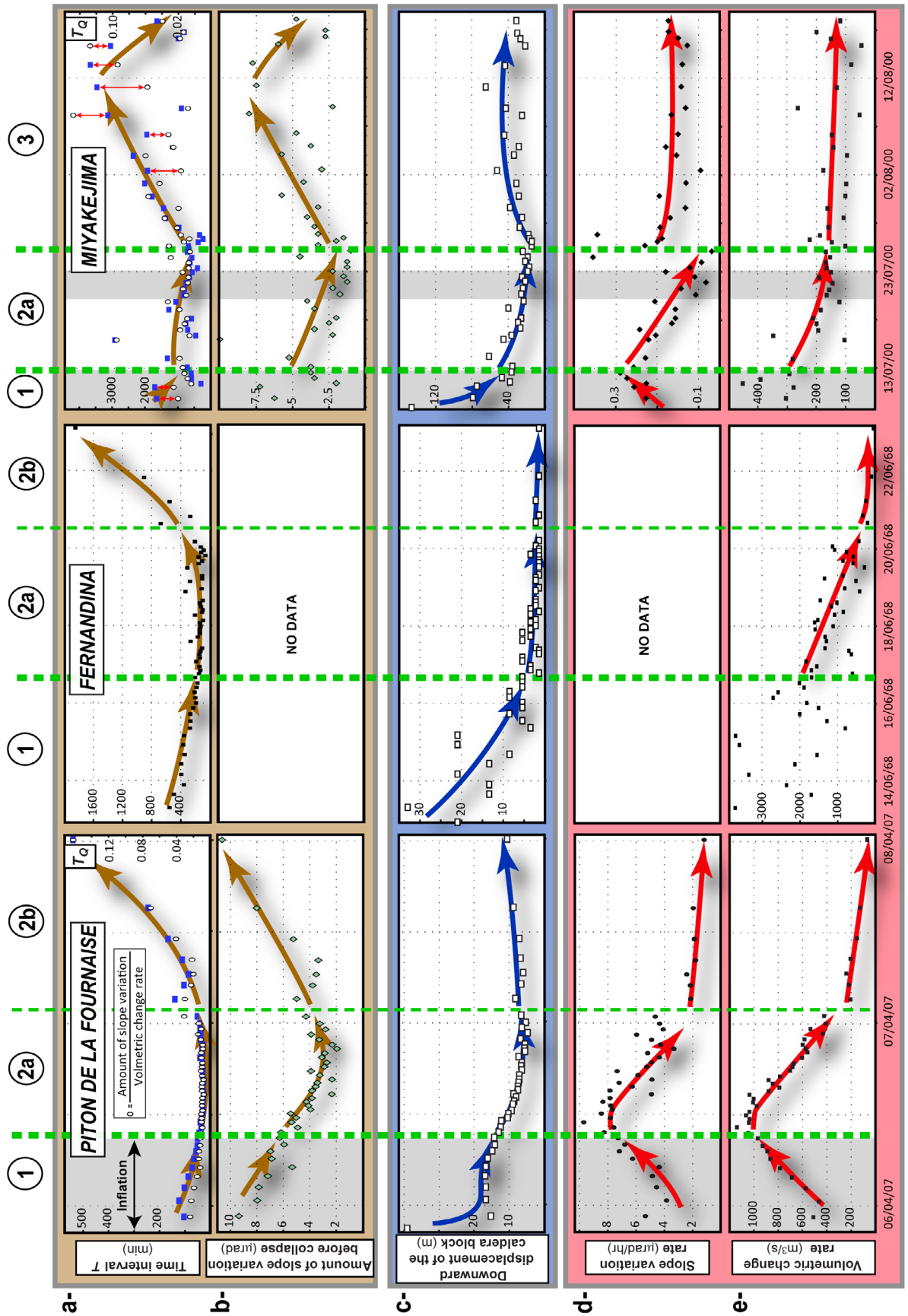

Figure 7. Comparison between the (a) time interval T between two collapses increments and T_Q, (b) amount of slope variation before collapse, (c) downward displacement of the caldera block, (d) slope variation rate and (e) volumetric change rate. See text for explanation. Red arrows in Figure 7a highlight the difference between T and T_Q for Miyakejima.

results from the influx of basaltic magmas within the 3-5-km-deep magma chamber of Miyakejima. Such an event could explain the composition change, from andesitic to basaltic, of the juveniles erupted on 14–15 July and 13 August [*Geshi and Oikawa*, 2008]. The influx-related overpressure could also explain the sudden augmentation of the edifice deformation rate by a higher rate of magma outflow, on 24 July, just after the inflation phase (Figure 7d).

[38] To conclude, data on Piton de la Fournaise and Miyakejima first show the striking effect of the collapsing rock column on the dynamics of the magma chamber and therefore on that of magma migration. The largest collapses trigger edifice inflation and boost the rate of magma outflow. The deformation of Miyakejima also suggests that influx of deeper magmas in the collapse-related reservoir may trigger edifice inflation during the development of collapse calderas.

6.3. Origin of T Variations

[39] Prior to this work, the evolution of T was described as being different for Piton de la Fournaise, Fernandina and Miyakejima, each volcano having a specific dynamics [*Filson et al.*, 1973; *Ukawa et al.*, 2000; *Michon et al.*, 2007; *Stix and Kobayashi*, 2008; *Staudacher et al.*, 2009]. We conversely showed from tiltmeter and seismic data that despite large differences in the caldera geometry and the duration of the whole collapse caldera processes, Piton de la Fournaise and Fernandina experienced a similar collapse dynamics, which contrasts with that of Miyakejima (Figure 2c).

[40] According to equation (1), T depends on (1) geometrical parameters defining to the size of the magma chamber V_0 and the surface of caldera block S, (2) the magma's bulk modulus κ, (3) the rate of magma withdrawal α, and (4) the frictional resistance $F_S - F_D$. κ and $F_S - F_D$ are considered as the two most prominent parameters controlling the collapse dynamics [*Simkin and Howard*, 1970; *Filson et al.*, 1973; *Kobayashi et al.*, 2003; *Stix and Kobayashi*, 2008].

[41] In the present work, the amount of slope variation before collapse gives insight into the evolution of the frictional resistance $F_S - F_D$ along the ring faults. Following *Kumagai et al.* [2001] and *Stix and Kobayashi* [2008], the volumetric change rate (Figure 7e) is considered as corresponding to the magma outflow rate. The other parameters involved in equation (1) being either unknown (κ) or constant (V_0 and S), we determined a time interval T_Q as the ratio between the amount of slope variation and the volumetric change rate for Piton de la Fournaise and Miyakejima (Figure 7a). The strikingly similar evolution of T and T_Q for Piton de la Fournaise indicates that (1) both parameters chiefly and equally controlled the time interval between two collapse increments and (2) κ did not significantly influenced T during the whole caldera collapse. Applying this result to Fernandina where the evolution of T is similar to that of Piton de la Fournaise (Figure 2c), we propose that the collapse dynamics in 1968 was also governed by $F_S - F_D$ and α.

[42] Comparison of T and T_Q for Miyakejima confirms the important role of α and $F_S - F_D$ in the collapse dynamics. However, the relatively large differences between T and T_Q for the two first collapses and during phase 3 suggest that T was not only controlled by the magma withdrawal rate and the frictional resistance (Figure 7a). Such a difference may result from a rapid increase of κ during the collapse process first 3 days and its decrease after 25 August. Assuming an andesitic magma richer in volatile than the basaltic one involved at Piton de la Fournaise and Fernandina, the magma underpressure that initiated the collapse of the caldera block likely triggered magma vesiculation and consequently a decrease of the bulk modulus, as described for silicic calderas [e.g., *Martí et al.*, 2000]. κ then increased when the pressure augmentation caused by the collapse of the rock column prevented any magma vesiculation. We propose that the decrease of κ after 25 July results from the influx of a deep volatile-rich basaltic magma into the collapse-related magma chamber. The presence of such magma has been evidenced by the huge SO_2 degassing since the 18 August summit eruption, which likely opened a pathway to the volatile phases to the surface [*Kazahaya et al.*, 2004].

[43] In summary, our data on Piton de la Fournaise and Miyakejima clearly show that the magma withdrawal rate is as important as the frictional resistance in the collapse dynamics in basaltic setting. Variations of the magma bulk modulus may also influence in a lesser extend this dynamics.

6.4. Synthetic Model for the Development of Basaltic Calderas

[44] Caldera collapses of Piton de la Fournaise, Fernandina and Miyakejima have showed that basaltic calderas are the result of successive collapse increments [*Simkin and Howard*, 1970; *Kumagai et al.*, 2001; *Michon et al.*, 2007].

[45] The present work enables quantification of the timing of collapse (i.e., the collapse dynamics), the downward displacements related to each collapse increment, the magma emission rates throughout the collapse caldera process. It also gives new insights into the collapse-related edifice deformation and the parameters controlling the collapse dynamics. Taking into account the 2 phases recognized at Piton de la Fournaise and Fernandina and a third one at Miyakejima, we propose the following synthetic evolution for the development of basaltic calderas:

[46] First of all, the basaltic volcano experiences a lateral intrusion fed by an intraedifice magma chamber. Magma withdrawal from the reservoir leads to a centripetal deflation until the rupture of the magma chamber roof [e.g., *Druitt and Sparks*, 1984].

[47] Phase 1 begins as soon as the caldera block collapses into the magma chamber. It is characterized by the largest collapse events, an incremental edifice inflation and a step-by-step increase of magma outflow. Edifice expansion and the augmentation of the magma withdrawal arise from a common source: the incremental overpressure caused by the volume of rock intruded in the magma chamber larger than that of magma withdrawn from the reservoir prior to the collapse. During this period the caldera block forcefully pushes the magma out of the reservoir. We propose that the decrease of the frictional resistance is caused by upward fluid migration along the ring faults, due to overpressure. Then, phase 1 is comparable to the period of increasing mass eruption rate described by *Martí et al.* [2000] and *Folch and Martí* [2009] for silicic calderas, once the piston subsidence starts (Figure 8).

[48] Phase 2 is characterized by a decrease of the rate of magma outflow, collapse increments of small amplitude and an edifice overall deflation. The constant deflation indicates

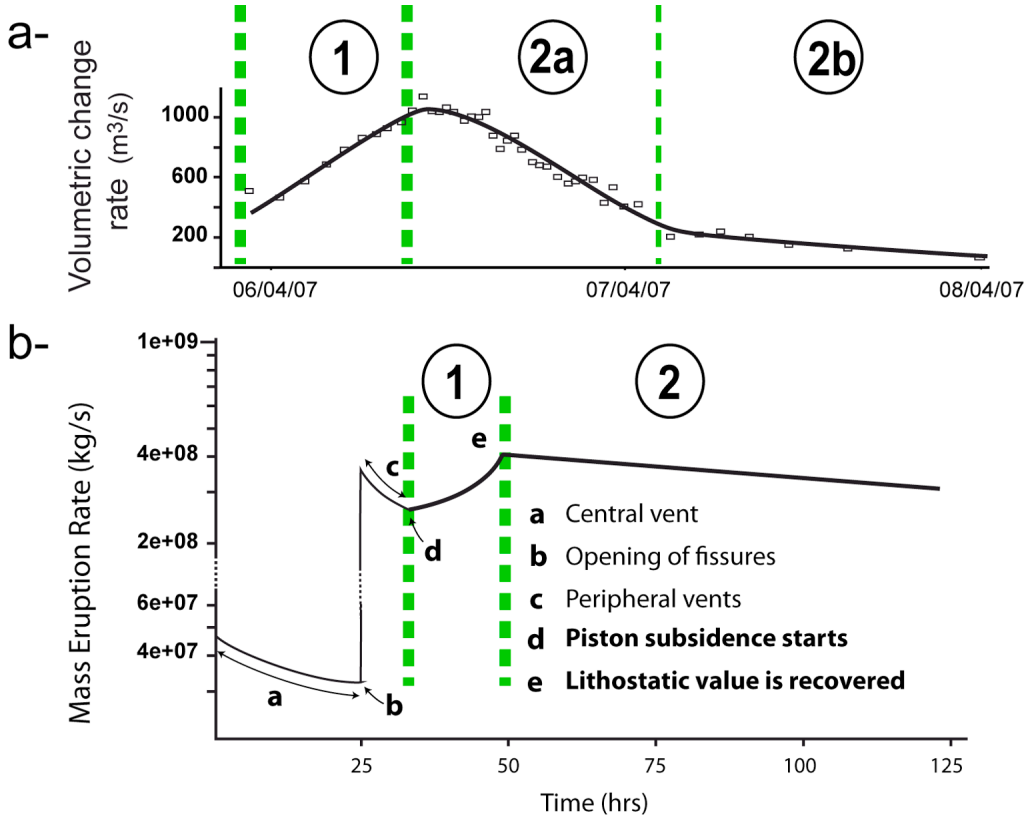

Figure 8. Twofold collapse dynamics for (a) basaltic and (b) silicic calderas. Figure 8a gives the rate of magma outflow determined for the caldera collapse of Piton de la Fournaise, while Figure 8b gives the mass eruption rate calculated by *Folch and Martí* [2009] for silicic calderas.

that the volume of material intruded in the magma chamber is lower than that of magma withdrawn from the reservoir. It therefore suggests that the caldera block ceases to push the magma out of the reservoir since the end of phase 1. We propose that the transition from phases 2a to 2b results from the increase of the frictional resistance along the ring faults, that could originates from a decrease of upward fluid migration when overpressure stops. As a whole, phase 2 shows striking similarities with the period of decreasing mass eruption rate described by *Folch and Martí* [2009] for silicic calderas (Figure 8). As a consequence, basaltic and silicic calderas are characterized by a first-order similar collapse dynamics despite large differences in the caldera geometry, magma compositions and eruption styles.

[49] Phase 3 is observed at Miyakejima only. It is marked by almost constant rates of both edifice deflation and magma outflow until the end of the caldera collapse. Such an evolution results from the influx volatile-rich deep magma in the collapse-related reservoir, which rejuvenates the collapse dynamics.

7. Conclusion

[50] Compiling GPS, tiltmeter and seismic data recorded during the caldera collapses of Fernandina, Miyakejima and Piton de la Fournaise [*Filson et al.*, 1973; *Ukawa et al.*, 2000; *Yamamoto et al.*, 2001; *Staudacher et al.*, 2009], we conclude that

[51] 1. The caldera collapse of Piton de la Fournaise and Fernandina are characterized by a similar collapse dynamics despite large differences in the caldera size and the roof aspect ratios. For both volcanoes, the magma outflow rate and the frictional resistance along the ring faults chiefly controlled the time interval evolution. This common evolution contrasts with that of Miyakejima where the collapse dynamics was influenced by the magma outflow rate, the frictional resistance along the ring faults and also by the magma bulk modulus and an influx of deep magma during the collapse caldera process.

[52] 2. The collapsing rock column pushes the magma out of the magma chamber during the first collapse increments only. These increments entailed overpressure in the magma chamber and consequently the edifice inflation and the increase of the magma evacuation rate.

[53] 3. The magma chamber roof collapsed for relatively small amounts of magma evacuated despite large roof aspect ratios (8.2%, 6.4% and 9.4% for Piton de la Fournaise, Fernandina and Miyakejima, respectively). Such low values may result from the continuous fluids migration along pre-existing ring faults that weaken the edifice strength and/or the gas-poor magma composition as already suggested by *Martí et al.* [2000].

[54] 4. Collapse caldera processes in basaltic setting are characterized by two successive phases. Phase 1 corresponds to a period of increasing magma withdrawal rates. According to GPS data recorded at Piton de la Fournaise

and Miyakejima, this phase is coeval with edifice inflation. Rates of magma outflow next decrease during phase 2 as the edifice deflates. The striking similarity between this evolution inferred for basaltic calderas and the twofold evolution described for silicic collapse calderas, i.e., increase then decrease of the mass eruption rate [*Folch and Martí*, 2009], suggests that basaltic and silicic calderas are both characterized by a first-order identical dynamics. If new magma is injected into the collapse-related reservoir then the collapse dynamics may slightly change as during phase 3 at Miyakejima.

[55] **Acknowledgments.** The authors thank Adelina Geyer and an anonymous reviewer for their helpful comments.

References

Aramaki, S. (1984), Formation of the Aira caldera, southern Kyushu, 22,000 years ago, *J. Geophys. Res.*, *89*, 8485–8501, doi:10.1029/JB089iB10p08485.

Bonafede, M. (1991), Hot fluid migration: An efficient source of ground deformation - Application to the 1982–1985 crisis at Campi Flegrei-Italy, *J. Volcanol. Geotherm. Res.*, *48*, 187–198, doi:10.1016/0377-0273(91)90042-X.

Cioni, R., R. Santacroce, and A. Sbrana (1999), Pyroclastic deposits as a guide for constructing the multi stage evolution of the Somma Vesuvius caldera, *Bull. Volcanol.*, *61*, 207–222, doi:10.1007/s004450050272.

Coppola, D., P. Piscopo, T. Staudacher, and C. Cigolini (2009), Lava discharge rate and effusive pattern of Piton de la Fournaise from MODIS data, *J. Volcanol. Geotherm. Res.*, *184*, 174–192, doi:10.1016/j.jvolgeores.2008.11.031.

Delaney, P. T., and D. F. McTigue (1994), Volume of magma accumulation or withdrawal estimated from surface uplift or subsidence, with application to the 1960 collapse of Kilauea volcano, *Bull. Volcanol.*, *56*, 417–424, doi:10.1007/BF00302823.

Dieterich, J. H., and R. W. Decker (1975), Finite element modeling of surface deformation associated with volcanism, *J. Geophys. Res.*, *80*, 4094–4102, doi:10.1029/JB080i029p04094.

Druitt, T. H., and C. R. Bacon (1989), Petrology of the zoned calcalkaline magma chamber of Mount Mazama, Crater Lake, Oregon, *Contrib. Mineral. Petrol.*, *101*, 245–259, doi:10.1007/BF00375310.

Druitt, T. H., and R. S. J. Sparks (1984), On the formation of calderas during ignimbrite eruptions, *Nature*, *310*, 679–681, doi:10.1038/310679a0.

Dvorak, J. J. (1992), Mechanism of explosive eruptions of Kilauea Volcano, Hawaii, *Bull. Volcanol.*, *54*, 638–645, doi:10.1007/BF00430777.

Dzurisin, D., K. M. Yamashita, and J. W. Kleinman (1994), Mechanisms of crustal uplift and subsidence at the Yellowstone caldera, Wyoming, *Bull. Volcanol.*, *56*, 261–270, doi:10.1007/BF00302079.

Filson, J., T. Simkin, and L.-K. Leu (1973), Seismicity of a caldera collapse: Galapagos Islands 1968, *J. Geophys. Res.*, *78*, 8591–8622, doi:10.1029/JB078i035p08591.

Folch, A., and J. Martí (2009), Time-dependent chamber and vent conditions during explosive caldera-forming eruptions, *Earth Planet. Sci. Lett.*, *280*, 246–253, doi:10.1016/j.epsl.2009.01.035.

Folch, A., R. Codina, and J. Martí (2001), Numerical modeling of magma withdrawal during explosive caldera-forming eruptions, *J. Geophys. Res.*, *106*(B8), 16,163–16,175, doi:10.1029/2001JB000181.

Gardner, J. E., and S. Tait (2000), The caldera forming eruption of Volcán Ceboruco, Mexico, *Bull. Volcanol.*, *62*, 20–33, doi:10.1007/s004450050288.

Geshi, N. (2009), Asymmetric growth of collapsed caldera by oblique subsidence during the 2000 eruption of Miyakejima, Japan, *Earth Planet. Sci. Lett.*, *280*, 149–158, doi:10.1016/j.epsl.2009.01.027.

Geshi, N., and T. Oikawa (2008), Phreatomagmatic eruptions associated with the caldera collapse during the Miyakejima 2000 eruption, Japan, *J. Volcanol. Geotherm. Res.*, *176*, 457–468, doi:10.1016/j.jvolgeores.2008.04.013.

Geshi, N., T. Shimano, T. Chiba, and S. Nakada (2002), Caldera collapse during the 2000 eruption of Miyakejima Volcano, Japan, *Bull. Volcanol.*, *64*, 55–68, doi:10.1007/s00445-001-0184-z.

Geyer, A., A. Folch, and J. Martí (2006), Relationship between caldera collapse and magma chamber withdrawal: An experimental approach, *J. Volcanol. Geotherm. Res.*, *157*, 375–386, doi:10.1016/j.jvolgeores.2006.05.001.

Irwan, M., F. Kimata, and N. Fujii (2006), Time dependent modeling of magma intrusion during the early stage of the 2000 Miyakejima activity, *J. Volcanol. Geotherm. Res.*, *150*, 202–212, doi:10.1016/j.jvolgeores.2005.07.014.

Ito, T., and S. Yoshioka (2002), A dike intrusion model in and around Miyakejima, Niijima and Kozushima in 2000, *Tectonophysics*, *359*, 171–187, doi:10.1016/S0040-1951(02)00510-3.

Kazahaya, K., H. Shinohara, K. Uto, M. Odai, Y. Nalkahori, H. Mori, H. Iino, M. Miyashita, and J. Hirabayashi (2004), Gigantic SO_2 emission from Miyakejima volcano, Japan, caused by caldera collapse, *Geology*, *32*, 425–428, doi:10.1130/G20399.1.

Kikuchi, M., Y. Yamanaka, and K. Koketsu (2001), Source process of the long-period seismic pulses associated with the 2000 eruption of Miyakejima volcano, and its implications, *J. Geogr.*, *110*, 204–216.

Kobayashi, T., T. Ohminato, and Y. Ida (2003), Earthquakes series preceding very long period seismic signals, observed during the 2000 Miyakejima volcanic activity, *Geophys. Res. Lett.*, *30*(8), 1423, doi:10.1029/2002GL016631.

Kumagai, H., T. Ohminato, M. Nakano, M. Ooi, A. Kubo, H. Inoue, and J. Oikawa (2001), Very-long-period seismic signals and the caldera formation at Miyake Island, Japan, *Science*, *293*, 687–690, doi:10.1126/science.1062136.

Lénat, J.-F., P. Bachèlery, A. Bonneville, and A. Hirn (1989), The beginning of the 1985–1987 eruptive cycle at Piton de la Fournaise (La Réunion): New insights in the magmatic and volcano-tectonic systems, *J. Volcanol. Geotherm. Res.*, *36*, 209–232, doi:10.1016/0377-0273(89)90015-2.

Martí, J., A. Folch, G. Macedonio, and A. Neri (2000), Pressure evolution during caldera forming eruptions, *Earth Planet. Sci. Lett.*, *175*, 275–287, doi:10.1016/S0012-821X(99)00296-4.

Michon, L., T. Staudacher, V. Ferrazzini, P. Bachèlery, and J. Martí (2007), April 2007 collapse of Piton de la Fournaise: A new example of caldera formation, *Geophys. Res. Lett.*, *34*, L21301, doi:10.1029/2007GL031248.

Michon, L., N. Villeneuve, T. Catry, and O. Merle (2009), How summit calderas collapse on basaltic volcanoes: New insights from the April 2007 caldera collapse of Piton de la Fournaise volcano, *J. Volcanol. Geotherm. Res.*, *184*, 138–151, doi:10.1016/j.jvolgeores.2008.11.003.

Murase, M., et al. (2006), Time dependent model of magma intrusion in and around Miyake and Kozu Islands, central Japan in June–August, 2000, *J. Volcanol. Geotherm. Res.*, *150*, 213–231, doi:10.1016/j.jvolgeores.2005.02.005.

Nakada, S., M. Nagai, T. Kaneko, A. Nozawa, and K. Suzuki-Kamata (2005), Chronology and products of the 2000 eruption of Miyakejima Volcano, Japan, *Bull. Volcanol.*, *67*, 205–218, doi:10.1007/s00445-004-0404-4.

Nishimura, T., S. Ozawa, M. Murakami, T. Sagiya, T. Tada, M. Kaizu, and M. Ukawa (2001), Crustal deformation caused by magma migration in the northern Izu Islands, Japan, *Geophys. Res. Lett.*, *28*, 3745–3748, doi:10.1029/2001GL013051.

Pallister, J. S., R. P. Hoblitt, G. P. Meeker, R. J. Knight, and D. F. Siems (1996), Magma mixing at mount Pinatubo: Petrologic and chemical evidence from the 1991 deposits, in *Fire and Mud: Eruptions and Lahars of Mount Pinatubo Philippines*, edited by C. G. Newhall and R. S. Punongbayan, pp. 687–732, Univ. of Wash. Press, Seattle.

Peltier, A., V. Famin, P. Bachèlery, V. Cayol, Y. Fukushima, and T. Staudacher (2008), Cyclic magma storages and transfers at Piton de La Fournaise volcano (La Réunion hotspot) inferred from deformation and geochemical data, *Earth Planet. Sci. Lett.*, *270*, 180–188, doi:10.1016/j.epsl.2008.02.042.

Pyle, D. M. (1990), New estimates for the volume of the Minoan eruption, in *Thera and the Aegean World III*, vol. 2, *Earth Sciences*, edited by D. A. Hardy, pp. 113–121, Thera Found., London.

Roche, O., and T. H. Druitt (2001), Onset of caldera collapse during ignimbrite eruptions, *Earth Planet. Sci. Lett.*, *191*, 191–202, doi:10.1016/S0012-821X(01)00428-9.

Roche, O., T. H. Druitt, and O. Merle (2000), Experimental study of caldera formation, *J. Geophys. Res.*, *105*, 395–416, doi:10.1029/1999JB900298.

Simkin, T., and K. A. Howard (1970), Caldera collapse in Galapagos Islands, 1968, *Science*, *169*, 429–437, doi:10.1126/science.169.3944.429.

Staudacher, T., V. Ferrazzini, A. Peltier, P. Kowalski, P. Boissier, P. Catherine, F. Lauret, and F. Massin (2009), The April 2007 eruption and the Dolomieu crater collapse, two major events at Piton de la Fournaise (La Réunion Island, Indian Ocean), *J. Volcanol. Geotherm. Res.*, *184*, 126–137, doi:10.1016/j.jvolgeores.2008.11.005.

Stix, J., and T. Kobayashi (2008), Magma dynamics and collapse mechanisms during four historic caldera-forming events, *J. Geophys. Res.*, *113*, B09205, doi:10.1029/2007JB005073.

Troise, C., F. Pingue, and G. De Natale (2003), Coulomb stress changes at calderas: Modeling the seismicity of Campi Flegrei (southern Italy), *J. Geophys. Res.*, *108*(B6), 2292, doi:10.1029/2002JB002006.

Ueda, H., E. Fujita, M. Ukawa, E. Yamamoto, M. Irwan, and F. Kimata (2005), Magma intrusion and discharge process at the initial stage of the 2000 activity of Miyakejima, central Japan, inferred from tilt and GPS data, *Geophys. J. Int.*, *161*, 891–906, doi:10.1111/j.1365-246X.2005.02602.x.

Ukawa, M., E. Fujita, E. Yamamoto, Y. Okada, and M. Kikuchi (2000), The 2000 Miyakejima eruption: Crustal deformation and earthquakes observed by the NIED Miyakejima observation network, *Earth Planets Space*, *52*, xix–xxvi.

Urai, M., N. Geshi, and T. Staudacher (2007), Size and volume evaluation of the caldera collapse on Piton de la Fournaise volcano during the April 2007 eruption using ASTER stereo imagery, *Geophys. Res. Lett.*, *34*, L22318, doi:10.1029/2007GL031551.

Villemant, B., A. Salün, and T. Staudacher (2009), Evidence for a homogeneous primary magma at Piton de la Fournaise (La Réunion): A geochemical study of matrix glass, melt inclusions and Pélé's hairs of the 1998–2008 eruptive activity, *J. Volcanol. Geotherm. Res.*, *184*, 79–92, doi:10.1016/j.jvolgeores.2009.03.015.

Wallace, P. J., A. T. Anderson Jr., and A. M. Davis (1999), Gradients in H_2O, CO_2, and exsolved gas in a large volume silicic magma system: Interpreting the record preserved in melt inclusions from the Bishop Tuff, *J. Geophys. Res.*, *104*, 20,097–20,122, doi:10.1029/1999JB900207.

Walsh, J. B., and R. W. Decker (1971), Surface deformation associated with volcanism, *J. Geophys. Res.*, *76*, 3291–3302, doi:10.1029/JB076i014p03291.

Wilson, R. M. (1935), Ground surface movement at Kilauea Volcano, *Hawaii Univ. Hawaii Res. Publ. 10*, 56 pp.

Wright, T. L., and S. Sakai (2004), Interpretation of the Miyakejima 2000 eruption and dike emplacement using time animations of earthquakes, *Bull. Earthquake Res. Inst. Univ. Tokyo*, *79*, 1–16.

Yamamoto, E., M. Ukawa, E. Fujita, Y. Okada, and M. Kikuchi (2001), Step-like tilt change occurred during the caldera-forming stage of the 2000 Miyakejima Volcanic Activity, *J. Geogr.*, *110*, 181–190.

V. Famin and L. Michon, Laboratoire GéoSciences Réunion, Université de la Réunion, 15 ave. René Cassin, F-97715 Saint Denis CEDEX 09, France. (laurent.michon@univ-reunion.fr)

V. Ferrazzini and F. Massin, Institut de Physique du Globe de Paris, Sorbonne Paris Cité, 1 rue Jussieu, F-75238 Paris CEDEX 05, France.

G. Roult, Seismology Department, Institut de Physique du Globe de Paris, Sorbonne Paris Cité, 1 rue Jussieu, F-75238 Paris CEDEX 05, France.